Letter

Stability of xenon-sodium compounds at moderately low pressures

Junhao Peng,[1,*] Shaoxiong Wang,[1,*] Huafeng Dong,[1,2,†] Minru Wen,[1] Xin Zhang,[1] and Fugen Wu[2,3]
[1]*School of Physics and Optoelectronic Engineering, Guangdong University of Technology, Guangzhou 510006, China*
[2]*Guangdong Provincial Key Laboratory of Information Photonics Technology, Guangdong University of Technology, Guangzhou 510006, China*
[3]*School of Materials and Energy, Guangdong University of Technology, Guangzhou 510006, China*

(Received 11 December 2023; accepted 8 April 2024; published 22 April 2024)

A growing body of theoretical and experimental evidence suggests that inert gases (He, Ne, Ar, Kr, Xe, Rn) become less and less inert under increasing pressure. Here we use crystal structure prediction software based on the *ab initio* evolutionary algorithm, named USPEX, to predict stable compounds of Xe and Na at pressures below 100 GPa, and we find three stable compounds, NaXe, $NaXe_3$, and $NaXe_4$. The NaXe belongs to a well-known cubic CsCl structure type. $NaXe_4$'s structure is common in amphiboles, whereas $NaXe_3$ has a unique structure, analogous to the "post-perovskite" orthorhombic $CaIrO_3$-type structure with Ir atoms removed. NaXe, $NaXe_3$, and $NaXe_4$ are found to be metallic.

DOI: 10.1103/PhysRevB.109.L140103

Inert (or "noble") gases have a closed valence shell—it is difficult to remove from or add to it an electron, or to share electrons with other atoms. This inertness decreases from light (He, Ne) to heavy (Xe, Rn) noble gases, and with increasing pressure. One may distinguish four situations:

(1) van der Waals compounds, which are stabilized under pressure because of denser packing of two (or more) atoms of different size. For example, at the pressure of 4.78 GPa, Somayazulu *et al.* discovered a stable Xe-H compound $Xe(H_2)_8$ [1].

(2) Neutral insertion of noble gases into ionic or electride structures. Examples are Na_2He [2] and Na_2OHe [3] and such compounds as CaF_2He and MgF_2He.

(3) Bonding with electronegative elements. For example, Xe forms stable fluorides already at ambient pressure [4], and stable oxides at pressures >74 GPa [5,6]—whereas He would require terapascal pressures to form stable compounds with F or O. There is evidence for incorporation of Xe into quartz (SiO_2) at rather low pressures (0.7–5 GPa) and elevated temperatures (500–1500 K) [7].

(4) Bonding with electropositive elements. For example, Xe forms stable compounds with Fe and Ni at 150–350 GPa [8].

Here we consider the latter situation, where a noble gas forms a stable compound with a highly electropositive element. A large electronegativity difference should stabilize such compounds. On the other hand, Xe should form such compounds more easily, as its outer electrons are more polarizable, i.e., more susceptible to external influence and more prone to chemical bonding. Indeed, at relatively low pressures of >43 GPa, we predict the stability of NaXe; $NaXe_3$ is predicted to appear at pressures >63 GPa and $NaXe_4$ is predicted to appear at pressures >82 GPa.

In our study, USPEX (universal structure predictor: evolutionary xtallography) [9] is used to predict unusual stable structures. It searches for the lowest enthalpy structure under pressures of 0, 50, 75, and 100 GPa, and can predict stable compounds and the element ratio of the structure. A number of applications illustrate its power [5,9–11]. In order to make the search more thorough, after obtaining the element ratio of the structure, continue to search for the fixed composition. The first-generation structures are randomly created, all structures relax under constant pressure and 0 K, and enthalpy is used as the fitness. The highest energy structures (40%) were discarded and another generation was created, 30% of which were random and 70% were from the lowest enthalpy structure through heredity, lattice mutation, and transmutation. In addition, in order to determine the thermodynamically stable structure, the enthalpy of formation of the structure was calculated:

$$\Delta H \text{ (per atom)} = \frac{H(\mathrm{Na}_x\,\mathrm{Xe}_y) - [xH(\mathrm{Na}) + yH(\mathrm{Xe})]}{x+y},$$

where $H(\mathrm{Na}_x\,\mathrm{Xe}_y)$, $H(\mathrm{Na})$, and $H(\mathrm{Xe})$ are enthalpies of $\mathrm{Na}_x\,\mathrm{Xe}_y$ (per formula), and of stable phases of sodium and xenon (per atom), respectively, at given pressure. Then, using these enthalpies of formation, the convex hull was constructed—a phase is deemed thermodynamically stable if it lies on the convex hull, i.e., is lower in enthalpy than any isochemical assemblage of other phases.

Structure relaxations were performed using the Perdew-Burke-Ernzerhof (PBE) functional [12] in the framework of the projector augmented wave (PAW) method [13], as implemented in the VASP code [14]. For Na atoms we used PAW pseudopotentials with 1.4 a.u. core radius and $2s^2\,2p^6\,3s^1$ electrons treated as valence. For Xe the core radius was 1.45 a.u. and $4s^2\,4p^6\,4d^{10}\,5s^2\,5p^6$ electrons were treated as

*These authors contributed equally to this work.
†hfdong@gdut.edu.cn

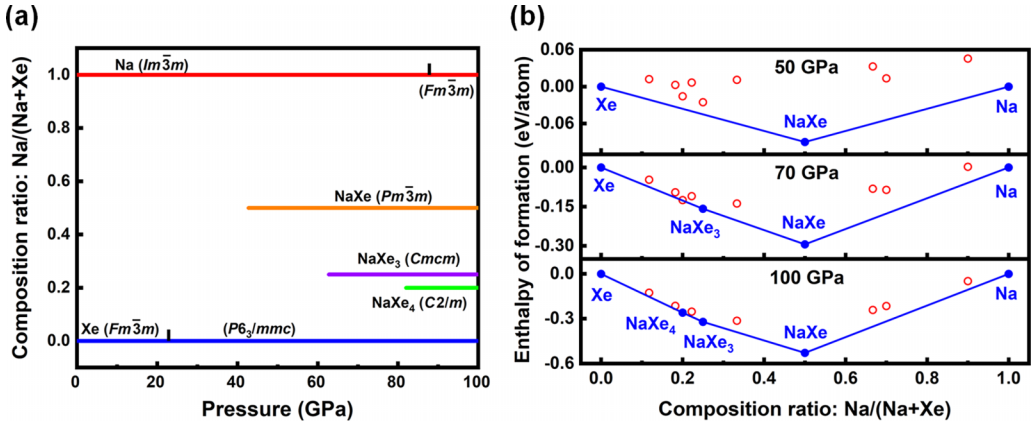

FIG. 1. Phase stability in the Na-Xe system. (a) Phase diagram of the Na-Xe system at a pressure of 0–100 GPa at a temperature of 0 K. (b) Convex hulls at pressures of 50, 70, and 100 GPa.

valence. We used a plane-wave kinetic energy cutoff of 800 eV, and sampled the Brillouin zone with uniform Γ-centered meshes of $2\pi \times 0.07\,\text{Å}^{-1}$ resolution within a structure search, and $2\pi \times 0.04\,\text{Å}^{-1}$ for subsequent highly precise relaxations and properties calculations. The structure parameters were fully optimized until the forces on each atom were less than 1×10^{-2} eV/Å. The energy convergence criterion for the electrons was set to be 1×10^{-8} eV. In order to judge the dynamical stability of the structure, the phonon spectra of $pm\bar{3}m$-NaXe (0 and 43 GPa), *Cmcm*-$NaXe_3$ (0 and 63 GPa), and $C2/m$-$NaXe_4$ (0 and 82GPa) were calculated with PHONOPY [15]. Bader charge analysis and partial charge density were used to analyze the charge transfer near the Fermi level. VASPKIT was used in data processing [16].

Figure 1(a) shows the phase diagram of the Na-Xe system in the pressure range 0–100 GPa. $pm\bar{3}m$-NaXe become stable at 43 GPa, *Cmcm*-$NaXe_3$ become stable at 63 GPa, and $C2/m$-$NaXe_4$ become stable at 82 GPa, respectively, and they remain stable at least up to 100 GPa (see Supplemental Material [17] for phase diagrams). Our phase diagram also shows predicted transitions in elemental Na (bcc to fcc), which has been reported before [10,18,19], and the phase transition in Xe (fcc to hcp), which is also known from experiments [20,21]. Figure 1(b) shows that the enthalpy of formation of NaXe, $NaXe_3$, and $NaXe_4$ becomes much more negative with pressure; i.e., these compounds become much more exothermic. One can also see that other stoichiometries, namely, Na_2Xe_{15}, Na_2Xe_9, $NaXe_2$, Na_2Xe, Na_9Xe, Na_7Xe_3, and Na_2Xe_7, come close to the convex hull and might become stable at pressures higher than 100 GPa. Phonon spectra calculations for $pm\bar{3}m$-NaXe, *Cmcm*-$NaXe_3$, and $C2/m$-$NaXe_4$ show no imaginary frequencies, indicating that compounds are dynamically stable in the pressure range of their stability. At ambient pressure all structures have imaginary phonon frequencies (see Supplemental Material [17] for phonon spectra), and are therefore not quenchable to ambient conditions.

Structural parameters of $pm\bar{3}m$-NaXe, *Cmcm*-$NaXe_3$, and $C2/m$-$NaXe_4$ are listed in Table I. $pm\bar{3}m$-NaXe has a well-known CsCl-type cubic structure [Fig. 2(a)], where atoms of both types have eightfold coordination. *Cmcm*-$NaXe_3$ has a very unusual structure [Fig. 2(c)], which can be derived from the $CaIrO_3$-type ("post-perovskite") structure [Fig. 2(d)] by

TABLE I. Lattice parameters and atomic coordinates for $Pm\bar{3}m$-NaXe (at 43 GPa), *Cmcm*-$NaXe_3$ (at 63 GPa), and $C2/m$-$NaXe_4$ (at 83 GPa).

			Wyckoff position				
Structure	Phase	Parameters (Å, deg)	Atom	Site	x	y	z
NaXe	$pm\bar{3}m$	$a = b = c = 3.282$	Na	b	0.500	0.500	0.500
		$\alpha = \beta = \gamma = 90$	Xe	a	0.000	0.000	0.000
$NaXe_3$	*Cmcm*	$a = b = 5.849$	Na	c	0.761	0.240	0.750
		$c = 8.302$					
		$\alpha = \beta = 90$	Xe	c	0.449	0.551	0.750
		$\gamma = 147.87$	Xe	f	0.135	0.865	0.556
$NaXe_4$	$C2/m$	$a = b = 5.642$	Na	i	0.821	0.821	0.692
		$c = 11.475$	Xe	i	0.866	0.866	0.305
		$\alpha = \beta = 112.25$					
			Xe	i	0.180	0.180	0.070
		$\gamma = 32.69$					
			Xe	i	0.384	0.384	0.543
			Xe	i	0.493	0.493	0.158

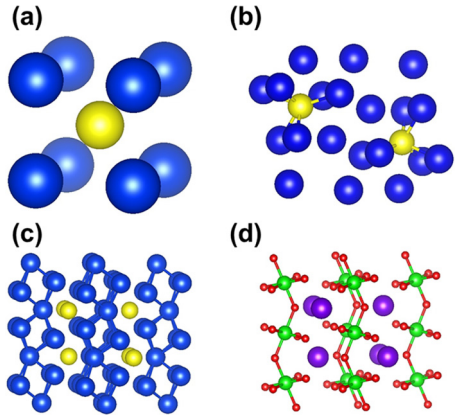

FIG. 2. Crystal structures of Na-Xe compounds. (a) $pm\bar{3}m$ -NaXe: the center of the cube is Na, and the eight atoms around it are Xe. (b) $C2/m$-$NaXe_4$: the blue ball is Xe and the yellow ball is Na. (c) $Cmcm$-$NaXe_3$: the blue ball is Xe and the yellow ball is Na. (d) $CaIrO_3$ (post-perovskite phase), in which the purple, red, and cyan spheres are Ca, O, and Ir atoms, respectively.

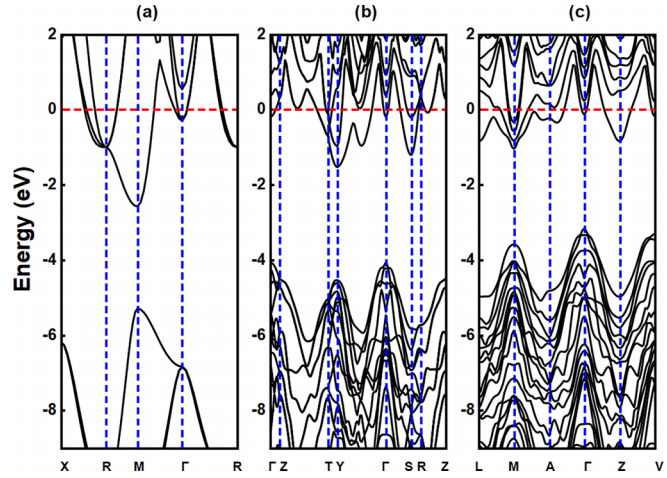

FIG. 3. Band structure of the structures. (a) Band structure of $pm\bar{3}m$-NaXe at a pressure of 43 GPa. (b) Band structure of $Cmcm$-$NaXe_3$ at a pressure of 63 GPa. (c) Band structure of $C2/m$-$NaXe_4$ at a pressure of 82 GPa. The energies have been aligned to place the Fermi level (E_F) at 0 eV.

removing the small cation (Ir). The $CaIrO_3$-type phase of $MgSiO_3$ (post-perovskite) is universally believed to be the main mineral phase of the Earth's lowermost mantle (the D″ layer) [22]. All known post-perovskite phases have ABX_3 stoichiometry; $Cmcm$-$NaXe_3$ is a post-perovskite phase with stoichiometry BX_3.

Cation-deleted versions of the perovskite structure are well known—deleting the large cation, one obtains the ReO_3 structure type. Deleting the small cation, one obtains the Cu_3Au structure, which is nothing but an ordered version of the cubic close-packed structure. $Cmcm$-$NaXe_3$ is an example of a cation-deleted version of a post-perovskite structure, with the deletion of the small cation. In this structure, each Na atom is coordinated by eight Xe atoms.

Calculated electronic band structures (Fig. 3) show that $pm\bar{3}m$ -NaXe, $Cmcm$-$NaXe_3$, and $C2/m$ − $NaXe_4$ are metallic: in NaXe three bands, in $NaXe_3$ four bands, and in $NaXe_4$ four bands cross the Fermi level. While NaXe has an odd number of electrons per unit cell and therefore has half-filled bands, $NaXe_3$ and $NaXe_4$ have an even number of electrons and could be insulators, yet are also metals. They all have band structure similar to n-doped semiconductors: there is a gap (∼2.7 eV) between fully occupied and partially filled bands. The latter can be viewed as electrons brought by the Na atoms and donated to the whole crystal.

In Fig. 4 we compare the calculated electronic densities of states of $pm\bar{3}m$-NaXe (43 GPa), $Cmcm$-$NaXe_3$ (63 GPa), and $C2/m$-$NaXe_4$ (82 GPa) with the densities of states obtained by removing Na atoms. One can see that removal of Na atoms makes the structures insulating, but we also see a considerable interaction of Na and Xe electrons in the energy range of [E_F-2eV, E_F] (E_F: Fermi level). In order to further explore the distribution of electrons that make the structure metallic, we calculated the partial charge densities of three structures (Fig. 5) in the energy range of [E_F-2eV, E_F]. The charge is mainly distributed between atoms. In $pm\bar{3}m$-NaXe (43 GPa), the charge is mainly distributed between Xe atoms; in $Cmcm$-$NaXe_3$ (63 GPa) and $C2/m$-$NaXe_4$ (82 GPa), the charge is mainly distributed on the connecting line of adjacent Na atoms. Although these electrons are jointly provided by Na and Xe atoms, we are curious about the main source of these electrons; thus we performed Bader analysis (Table II) [23–26]. This analysis shows that each Na atom loses 0.69 electrons in $pm\bar{3}m$-NaXe, 0.74 electrons in $Cmcm$-$NaXe_3$, and 0.76 electrons in $C2/m$-$NaXe_4$. In the Na-Xe system, when the proportion of Na increases (e.g., the metastable Na_3Xe_7 and Na_9Xe appearing on the convex hull), the system displays a feature of electrides. This feature can be visualized by the electron localization function (ELF). As shown in Fig. 6, the interstices among Na atoms in the Na_9Xe structure form highly localized electrons that exhibit anionlike behavior. This feature is also observed in the system of Na_3Xe_7

TABLE II. Bader analysis.

$pm\bar{3}m$-NaXe (43 GPa) charge transfer situation	
Atom	Charge
Na	+0.69
Xe	–0.69
$Cmcm$-$NaXe_3$ (63 GPa) charge transfer situation	
Atom	Charge
Na	+0.74
Xe	–0.24
Xe	–0.25
Xe	–0.25
$C2/m$-$NaXe_4$ (82 GPa) charge transfer situation	
Atom	Charge
Na	+0.76
Xe	–0.22
Xe	–0.12
Xe	–0.24
Xe	–0.18

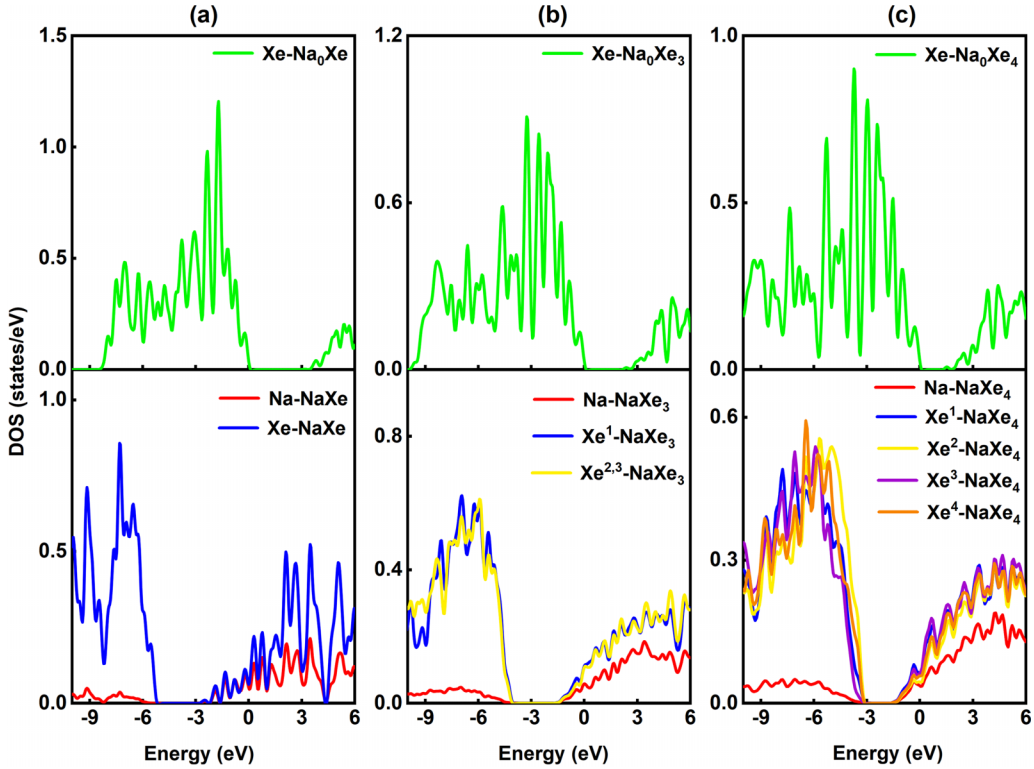

FIG. 4. Density of states of the structures. (a) Density of states of $pm\bar{3}m$-NaXe at 43 GPa. (b) Density of states of *Cmcm*-$NaXe_3$ at 63 GPa. (c) Density of states of *Cmcm*-$NaXe_4$ at 82 GPa. The density of states of elemental Xe under corresponding pressure is also added. The energies have been aligned to place the Fermi level (E_F) at 0 eV.

[Figs. 6(c) and 6(d)]. In contrast, for systems with a greater proportion of Xe, Na-Xe exhibits pronounced ionicity due to Xe being less and less inert under increasing pressure (Fig. S10 [17]), in which case the electrons lost from Na can be fully accepted by Xe. When the proportion of Xe decreases, it cannot fully accept the electrons lost from Na, and the electrons tend to be localized in the lattice interstices. The difference between the Na-Xe system and the Na-He system is that the Na-Xe system shows both electrides and ionic compounds at 100 GPa, due to Xe being less inert than He under pressure (it should be emphasized that Na_9Xe or Na_3Xe_7—which have the characteristics of electrides at 100 GPa—are metastable structures, and these structures tend to form stable compounds when the pressure is further increased, as shown in Fig. 1(b) and in the report of Zou *et al.* [27]).

In summary, by employing the evolutionary algorithm with USPEX, we have predicted some stable compounds in the Na-Xe system in the pressure range 0–100 GPa: $pm\bar{3}m$-NaXe (stable at >43 GPa and up to at least 100 GPa), *Cmcm*-$NaXe_3$ (stable at >63 GPa and up to at least 100 GPa), and

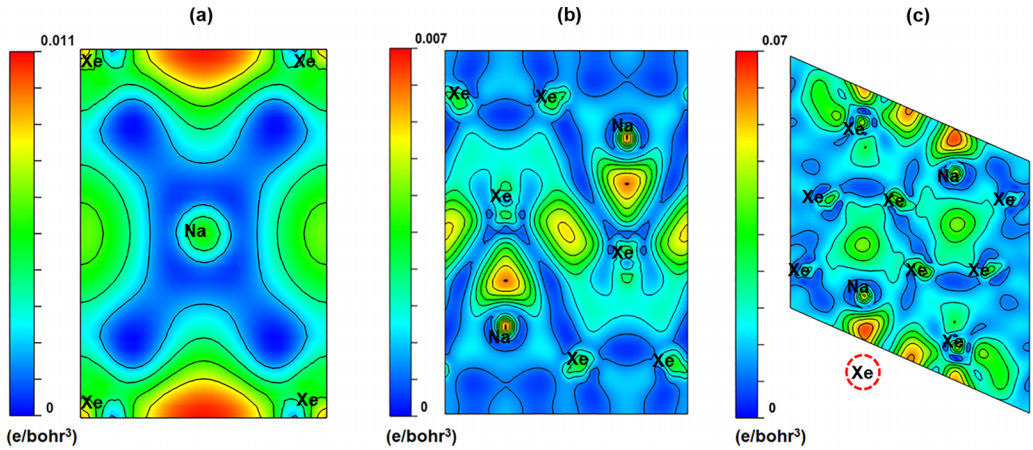

FIG. 5. Partial charge density in the energy range of [E_F-2eV, E_F] of three structures. The charge density is expressed in e/bohr^3. The sections of $pm\bar{3}m$-NaXe (43 GPa) and *Cmcm*-$NaXe_3$ (63 GPa) are (1 1 0), and the section of $C2/m$-$NaXe_4$ (82 GPa) is (–1 1 0).

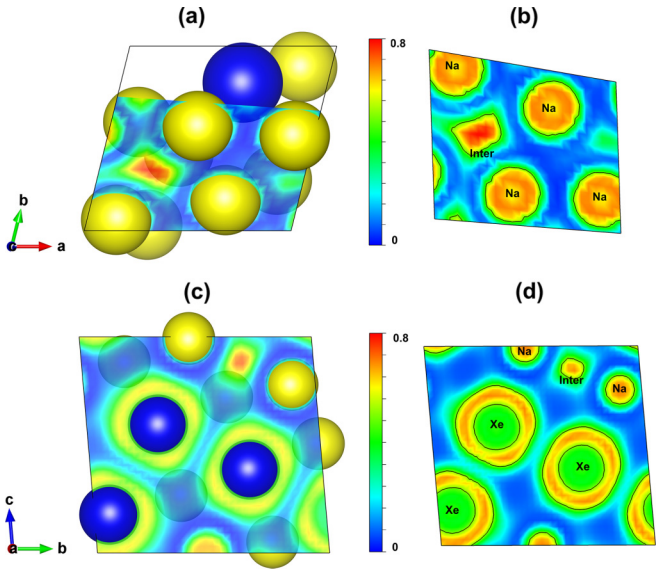

FIG. 6. (a) Crystal structure and (b) the 2D ELF corresponding to the slice plane of Na_9Xe at 100 GPa. (c) Crystal structure and (d) the 2D ELF corresponding to the slice plane of Na_3Xe_7 at 100 GPa.

$C2/m$-$NaXe_4$ (stable at >82 GPa and up to at least 100 GPa). $NaXe_3$ has a unique structure related to post-perovskite $CaIrO_3$-type structure. Electronic structure calculations suggest that $pm\bar{3}m$-NaXe, $Cmcm$-$NaXe_3$, and $C2/m$-$NaXe_4$ are metals. According to Bader analysis, electrons in the sodium atoms are transferred to the Xe atoms. The Xe atoms do not behave as fully inert; instead, the electrons of Na and Xe are coupled, and we see Xe atoms polarizing towards neighboring Na atoms in $Cmcm$-$NaXe_3$. Despite becoming stable at relatively low pressures, NaXe, $NaXe_3$, and $NaXe_4$ will not survive decompression to ambient pressure.

This work is supported by the National Natural Science Foundation of China (Grants No. 11604056, and No. 11804057) and the special fund for the climbing program of Guangdong Province, China. We thank the Center of Campus Network and Modern Educational Technology, Guangdong University of Technology, Guangdong, China for providing computational resources and technical support for this work. Many thanks to Prof. Artem R. Oganov, Prof. Alexander F. Goncharov, and Dr. Lin Wang for their useful discussions.

[1] M. Somayazulu, P. Dera, J. Smith, and R. J. Hemley, Structure and stability of solid $Xe(H_2)_n$, J. Chem. Phys. **142**, 104503 (2015).
[2] X. Dong, A. R. Oganov, A. F. Goncharov, E. Stavrou, S. Lobanov, G. Saleh, G.-R. Qian, Q. Zhu, C. Gatti, V. L. Deringer *et al.*, A stable compound of helium and sodium at high pressure, Nat. Chem. **9**, 440 (2017).
[3] Z. Liu, J. Botana, A. Hermann, S. Valdez, E. Zurek, D. Yan, H.-Q. Lin, and M.-S. Miao, Reactivity of He with ionic compounds under high pressure, Nat. Commun. **9**, 951 (2018).
[4] K. O. Christe, Bartlett's discovery of noble gas fluorides, a milestone in chemical history, Chem. Commun. **49**, 4588 (2013).
[5] Q. Zhu, D. Y. Jung, A. R. Oganov, C. W. Glass, C. Gatti, and A. O. Lyakhov, Stability of xenon oxides at high pressures, Nat. Chem. **5**, 61 (2013).
[6] A. Dewaele, N. Worth, C. J. Pickard, R. J. Needs, S. Pascarelli, O. Mathon, M. Mezouar, and T. Irifune, Synthesis and stability of xenon oxides Xe_2O_5 and Xe_3O_2 under pressure, Nat. Chem. **8**, 784 (2016).
[7] C. Sanloup, B. C. Schmidt, E. M. C. Perez, A. Jambon, E. Gregoryanz, and M. Mezouar, Retention of xenon in quartz and Earth's missing xenon, Science **310**, 1174 (2005).
[8] L. Zhu, H. Liu, C. J. Pickard, G. Zou, and Y. Ma, Reactions of xenon with iron and nickel are predicted in the Earth's inner core, Nat. Chem. **6**, 644 (2014).
[9] A. R. Oganov and C. W. Glass, Crystal structure prediction using *ab initio* evolutionary techniques: Principles and applications, J. Chem. Phys. **124**, 244704 (2006).
[10] Y. Ma, M. Eremets, A. R. Oganov, Y. Xie, I. Trojan, S. Medvedev, A. O. Lyakhov, M. Valle, and V. Prakapenka, Transparent dense sodium, Nature (London) **458**, 182 (2009).
[11] W. Zhang, A. R. Oganov, A. F. Goncharov, Q. Zhu, S. E. Boulfelfel, A. O. Lyakhov, E. Stavrou, M. Somayazulu, V. B. Prakapenka, and Z. Konôpková, Unexpected stable stoichiometries of sodium chlorides, Science **342**, 1502 (2013).
[12] J. P. Perdew, K. Burke, and M. Ernzerhof, Generalized gradient approximation made simple, Phys. Rev. Lett. **77**, 3865 (1996).
[13] P. E. Blöchl, Projector augmented-wave method, Phys. Rev. B **50**, 17953 (1994).
[14] G. Kresse and J. Furthmüller, Efficiency of *ab-initio* total energy calculations for metals and semiconductors using a plane-wave basis set, Comput. Mater. Sci. **6**, 15 (1996).
[15] L. Chaput, A. Togo, I. Tanaka, and G. Hug, Phonon-phonon interactions in transition metals, Phys. Rev. B **84**, 094302 (2011).
[16] V. Wang, N. Xu, J.-C. Liu, G. Tang, and W.-T. Geng, VASPKIT: A user-friendly interface facilitating high-throughput computing and analysis using VASP code, Comput. Phys. Commun. **267**, 108033 (2021).
[17] See Supplemental Material at http://link.aps.org/supplemental/10.1103/PhysRevB.109.L140103 for the phase diagram, phonon spectra, and electron localization function (ELF) of the system described in Fig. 1, and details of lattice parameters and atomic coordinates used in Fig. 6.
[18] M. Hanfland, I. Loa, and K. Syassen, Sodium under pressure: bcc to fcc structural transition and pressure-volume relation to 100 GPa, Phys. Rev. B **65**, 184109 (2002).
[19] D. N. Polsin, A. Lazicki, X. Gong, S. J. Burns, F. Coppari, L. E. Hansen, B. J. Henderson, M. F. Huff, M. I. Mcmahon, M. Millot *et al.*, Structural complexity in ramp-compressed sodium to 480 GPa, Nat. Commun. **13**, 2534 (2022).
[20] W. A. Caldwell, J. H. Nguyen, B. G. Pfrommer, F. Mauri, S. G. Louie, and R. Jeanloz, Structure, bonding, and geochemistry of xenon at high pressures, Science **277**, 930 (1997).
[21] H. Cynn, C. Yoo, B. Baer, V. Iota-Herbei, A. McMahan, M. Nicol, and S. Carlson, Martensitic fcc-to-hcp transformation observed in xenon at high pressure, Phys. Rev. Lett. **86**, 4552 (2001).

[22] A. R. Oganov and S. Ono, Theoretical and experimental evidence for a post-perovskite phase of $MgSiO_3$ in Earth's D″ layer, Nature (London) **430**, 445 (2004).

[23] G. Henkelman, A. Arnaldsson, and H. Jónsson, A fast and robust algorithm for Bader decomposition of charge density, Comput. Mater. Sci. **36**, 354 (2006).

[24] E. Sanville, S. D. Kenny, R. Smith, and G. Henkelman, Improved grid-based algorithm for Bader charge allocation, J. Comput. Chem. **28**, 899 (2007).

[25] W. Tang, E. Sanville, and G. Henkelman, A grid-based Bader analysis algorithm without lattice bias, J. Phys.: Condens. Matter **21**, 084204 (2009).

[26] M. Yu and D. R. Trinkle, Accurate and efficient algorithm for Bader charge integration, J. Chem. Phys. **134**, 064111 (2011).

[27] M. Zou, K. Yang, P. Zhang, W. Cui, J. Hao, J. Shi, and Y. Li, Existence of solid Na–Xe compounds at the extreme conditions of Earth's interior, Phys. Rev. Res. **5**, 043107 (2023).